Journal of Fundamental and Applied Research **Vol. 2**, Issue 3 (2022) 20220019

Received: 13 July 2022 / Accepted: 17 August 2022
Published online: 25 September 2022
© 2022 The Author(s)

Scalar field around stringy black hole

Bobir Toshmatov,[1,2,3,*] Azamjon Boydedayev,[4] and Sarvarbek Tojiev[5]

[1]*Ulugh Beg Astronomical Institute, Astronomy str. 33, Tashkent 100052, Uzbekistan*
[2]*New Uzbekistan University, Mustaqillik ave. 54, Tashkent 100007, Uzbekistan*
[3]*Institute of Nuclear Physics, Ulugbek 1, Tashkent 100214, Uzbekistan*
[4]*Faculty of Physics, Namangan State University, Uychi str. 316, Namangan 160136, Uzbekistan*
[5]*Academic Lyceum of the Tashkent State University of Transport, Tashkent 100067, Uzbekistan*

We study behaviour of massless and massive scalar test fields around stringy black holes and compare the results to those related to Reissner-Nordström black holes. We shown that the stringy and Reissner-Nordström black holes have similar influence on the behaviour of the scalar fields if their dimensionless charge parameter is small enough ($\lesssim 0.5$). The charge of the stringy and Reissner-Nordström black holes increases the frequency of quasinormal oscillations and damping rate as well. We shown that mass of the scalar field makes the quasinormal modes longer lived. However, quasinormal modes can only occur in a restricted region of the mass parameter of the scalar field and the charge parameter of the spacetime. Outside this parameter region, the quasinormal modes disappear. We also shown that around stringy black holes scalar fields are stable. Moreover, we shown that both stringy and Reissner-Nordström black holes are better reflectors than the Schwarzschild black holes. We demonstrate that damping of scalar quasinormal modes in stringy black hole spacetimes is suppressed in comparison to the Reissner-Nordström and Schwarzschild spacetimes.

I. INTRODUCTION

Black holes (BHs) are considered by General Relativity as objects that have so intense gravitational field that even light cannot escape from them. However, these objects also emit energy due to perturbations that come from the interactions of them with surrounding fields. BHs respond to the perturbations by emitting gravitational waves that can be treated as test fields not influencing the BH spacetimes [1]. The evolution of perturbations in BH spacetimes involves three stages [2]: (i) initial wave burst; (ii) the damped oscillations with complex frequencies-these frequencies are independent of the initial conditions and depend only on the BH spacetime characteristics as the mass, charge and the internal angular momentum (spin). These oscillations correspond to the so-called quasinormal modes (QNMs); (iii) the power-law tail behaviour of the waves at very late times.

One of the reasons of importance of studying the QNMs is that the test gravitational waves carry important information about BHs. By detecting them one can find the characteristic parameters of the BH spacetimes. Characteristic parameters of the BH spacetimes are also imprinted into behaviour of other test fields, as scalar and electromagnetic fields. Here we focus our attention to the simplest case of the scalar fields when also the massive field is usually considered [3].

So far, many works have been done in order to compute the QNMs (for comprehensive reviews see [4–7] and references therein). All studies have shown that perturbative studies of test fields on stationary backgrounds lead to a Schrödinger-like wave equation with complex frequency and a specific effective potential. However, it is impossible to solve this equation analytically even in the Schwarzschild BH case [8]. Therefore this equation is solved using semianalytical and numerical methods. The Reissner-Nordström (RN) BH case is more or less similar to the Schwarzschild case [9–14]. So far QNMs of the RN BH were calculated by several methods [4–7]. WKB (Wentzel-Kramers-Brillouin) method was applied for the first time for calculations of QNMs of the RN BH by Kokkotas and Schutz [9]. Weakly damped modes of massive charged fields were computed by the WKB method in [14]. Afterwards, in order to increase accuracy, the WKB method was extended to the third order by Iyer and

* toshmatov@astrin.uz

Will [15] and to the sixth order by Konoplya [16]. Calculation of the QNMs is possible also by the continued-fraction method that was applied for the first time for the RN BH by Leaver [10].

Nowadays, it seems that string theory is the most favourite candidate for consistent quantum theory of gravitation. In reality, BHs are never in an isolated state- they always have interactions with the surrounding (matter fields). Therefore, being based on the system of interactions of gravity + electromagnetic field + dilatonic field, in 1988 the first static spherically symmetric dilaton BH solution in the low-energy effective theory of heterotic strings in four dimensions was obtained by Gibbons and Maeda [17] and few years later by Garfinkle, Horowitz, and Strominger [18]. This dilaton BH solution is somewhat similar to the RN one with the added complexity of the effects of an additional dilaton field coupling. In the papers [19, 20] axial and polar perturbations of the charged, dilaton BH has been studied and shown in [20] that the isospectrality of axial and polar perturbations that characterizes both Schwarzschild and RN BHs is broken due to the presence of the dilaton. In the papers [21–23] scalar, Dirac and asymptotic QNMs of the stringy BH were studied. In the case of these fields being taken into account, the corresponding BHs are usually called "dirty" BHs. In the papers [24–27] QNMs of the dirty, dilatonic and quintessence BHs have been studied.

Although most studies of QNMs have been motivated by their astrophysical relevance, there are several other reasons to be interested in understanding the spectrum of oscillations of a BH. In particular, the QNMs play a crucial role in discussions of BH stability and the scattering problem. If a BH is unstable against small perturbations, it could be destroyed by them and the assumption of test field cannot be relevant. Recently, Li [28] shown by analyzing superradiant modes that the stringy BH is stable against the massive charged scalar perturbation. However, superradiant instability can be observed by adding the mirror-like boundary condition to the system of charged stringy BH [29]. Furthermore, in the papers [30–33], some properties of the dilatonic and RN BHs, such as superradiance, instability of the charged massive scalar field, and some other properties have been studied. Greybody factor and Hawking radiation of the stringy BH were studied by Kim and Oh [34] for the large BH limit ($\omega \ll 1/r_H$) by using semi-classical method. Moreover, in the papers [35–44] some methods of studying stability and greybody factor of charged, static, spherically symmetric BHs have been studied.

In this paper we aim to study the QNMs of the scalar field in the spacetimes of the stringy BHs, the stability and scattering of the scalar fields. For calculations of the QNMs we use the sixth order WKB method. This paper is organized as follows: Section II gives brief description about stringy BH. In section III dynamics of the scalar field of the stringy and RN BHs have been studied and their effective potentials are compared. Massless and massive QNMs of the stringy and RN BHs have been calculated by the sixth order WKB method in section IV. In section V we study the QNMs of the stringy and RN BHs in an eikonal limit (in large value of multipole number ℓ). In sections VI and VII stability and greybody factors of both BHs, respectively have been studied and compared with each other. Finally, in section VIII we present some concluding remarks. Throughout this work we use $G = c = \hbar = 1$, and metric signature $(-,+,+,+)$.

II. STRINGY BLACK HOLES

We can write the spacetime line element of the BH spacetime in the general form

$$ds^2 = -f(r)dt^2 + f^{-1}(r)dr^2 + g(r)d\Omega^2 \,, \tag{1}$$

with $d\Omega^2 = d\theta^2 + \sin^2\theta d\phi^2$. For the static spherically symmetric charged black holes in low energy effective theory of heterotic strings in four dimensions, the metric functions $f(r)$ and $g(r)$ are defined by the expressions [18]

$$f(r) = 1 - \frac{2M}{r} \,, \quad g(r) = r^2\left(1 - \frac{Q^2}{Mr}\right) \,, \tag{2}$$

where M and Q are mass and charge parameters of the stringy BH, respectively.

One can see from the spacetime metric of the stringy BH (1) and (2) that the event horizon of the stringy BH is located at $r = 2M$. In order to find the curvature singularity of the stringy BH we calculate the Kretschmann scalar

$$K = R_{\mu\nu\rho\sigma}R^{\mu\nu\rho\sigma} = \frac{W(M,r,Q)}{r^6(Q^2 - Mr)^4}, \tag{3}$$

where $W(M,r,Q)$ is some polynomial function of r, M and Q. One can see easily from the Kretschmann scalar (3) that the stringy BH has the curvature singularities at $r = 0$ and $r = Q^2/M$. This implies that an infalling particle, before hitting the $r = 0$ singularity, reaches the physical singularity at $r = Q^2/M$. This singularity can be located at arbitrary $r > 0$, depending on the values of charge Q and mass M. For $Q^2/M > 2M$, the event horizon of the stringy BH is surrounded by this singular surface and the spacetime describes a naked singularity. For $Q^2/M < 2M$, the singular surface is located inside the event horizon and we have a BH solution. In this paper we consider the second (BH) case.

Copyright © 2022

For convenience we turn into the following dimensionless quantities: $t/M \to t$, $r/M \to r$ and $Q/M \to q$. Then we rewrite the stringy spacetime metric (1) with new dimensionless coordinates and parameter q as

$$ds_s^2 = -\left(1-\frac{2}{r}\right)dt^2 + \left(1-\frac{2}{r}\right)^{-1}dr^2 + r^2\left(1-\frac{q^2}{r}\right)d\Omega^2 \,. \tag{4}$$

We shall compare the results for the stringy spacetimes to those obtained for the standard RN spacetimes with the line element given in the dimensionless form by

$$ds_{RN}^2 = -f_{RN}(r)dt^2 + f_{RN}^{-1}(r)dr^2 + r^2 d\Omega^2 \,, \tag{5}$$

with

$$f_{RN}(r) = 1 - \frac{2}{r} + \frac{e^2}{r^2} \,, \tag{6}$$

where e denotes the dimensionless RN charge parameter.

III. DYNAMICS OF SCALAR FIELD

Scalar field Φ is governed by the Klein-Gordon equation

$$\left[\frac{1}{\sqrt{-g}}\partial_\mu\left(\sqrt{-g}g^{\mu\nu}\partial_\nu\right) + m^2\right]\Phi = 0 \,, \tag{7}$$

where m is the mass of the scalar field. In a curved spacetime of spherically symmetric BH, $g^{\mu\nu}$ is the inverse metric tensor describing the spacetime in which the field propagates, ∂_μ is the partial derivative, and $-g$ is the absolute value of the determinant of the spacetime metric (4) and (6) that read

$$g_s = -r^4(1-q^2/r)^2\sin^2\theta \,, \qquad g_{RN} = -r^4\sin^2\theta. \tag{8}$$

In order to reduce the Klein-Gordon equation (7) into the two dimensional wave equation, we assume the scalar field separated in the standard form

$$\Phi(t,r,\theta,\phi) = \frac{1}{r}R(r,t)Y_\ell^m(\theta,\phi) \tag{9}$$

where $Y_\ell(\theta,\phi)$ is the so called spherical harmonic function of degree ℓ related to the angular coordinates θ,ϕ, and it fulfills the relation

$$\nabla^2_{\theta,\phi}Y_\ell^m(\theta,\phi) = -\ell(\ell+1)Y_\ell^m(\theta,\phi) \,. \tag{10}$$

A. Regge-Wheeler equation

Inserting the separated scalar function (9) into (7), we obtain the Regge-Wheeler wave equation relating the time and radial dependence of the scalar function

$$\left[\frac{\partial^2}{\partial t^2} - \frac{\partial^2}{\partial r_*^2} + V(r)\right]R(r,t) = 0. \tag{11}$$

In the Regge-Wheeler equation, r_* is the so-called tortoise radial coordinate defined by

$$dr_* = \frac{dr}{f(r)}. \tag{12}$$

Since $f(r)$ is the lapse function governing the event horizon location, r_* approaches $-\infty$ as r approaches the event horizon of the BH from infinity, thus

$$r_* \in (-\infty,+\infty) \,, \quad for \quad r \in (r_+,+\infty). \tag{13}$$

Copyright © 2022

Therefore, the Regge-Wheeler wave-like equation (11) will be restricted here only to the regions located outside the event horizon, $r > r_+$.

The effective potential $V(r)$ in the expression (11) depends on the specific field under consideration. For the massive scalar fields, the effective potential $V(r)$ of the stringy BH reads

$$V_s(r) = f(r)\left[\frac{\ell(\ell+1)}{r(r-q^2)} - f(r)\frac{q^4}{4r^2(r-q^2)^2} + f'(r)\frac{2r-q^2}{2r(r-q^2)} + m^2\right] \tag{14}$$

where parameter ℓ related to the spherical harmonics represents the orbital angular momentum and takes only non-negative integer values, $f'(r) = df(r)/dr$.

For the RN BH spacetime, the effective potential for the scalar field reads

$$V_{RN}(r) = f_{RN}(r)\left[\frac{\ell(\ell+1)}{r^2} + \frac{f'_{RN}(r)}{r} + m^2\right]. \tag{15}$$

In Fig. 1 and Fig. 2 some properties of the effective potentials of the stringy and RN BHs are illustrated. One can see from the Fig. 1 and Fig. 2 that the charges q and e, and the mass of the field m, increase the height of the effective potential.

In order to solve the Regge-Wheeler differential equation (11), we separate the r, t variables in the wave function assuming

$$R(r,t) = \psi(r)\xi(t)\,. \tag{16}$$

Putting the separated function (16) into (11), using the stationarity of the spacetime, and considering a wave incoming from infinity towards the BH,

$$\xi(t) \sim e^{-i\omega t}, \tag{17}$$

we obtain the radial part of the Regge-Wheeler wave equation in the form of the standard Schrödinger equation

$$\frac{d^2\psi(r)}{dr_*^2} + \left[\omega^2 - V(r)\right]\psi(r) = 0\,. \tag{18}$$

Calculation of the QNMs in black hole backgrounds requires the solution of Schrödinger-like wave equation with a particular boundary condition. Considering the boundary condition for an incoming wave at the event horizon, one can see from Fig. 1 that for $r \to r_+$ ($r_* \to -\infty$), the effective potential tends to zero, $V_{eff} \to 0$, therefore, in this limit, the incoming wave function $\psi(r)$ behaves as

$$\psi(r) \sim e^{-i\omega r_*} \quad as \quad r \to r_+ \quad (r_* \to -\infty). \tag{19}$$

One can see from the Fig. 1 that the effective potential (14) does not vanish at the spatial infinity $r \to +\infty$ ($r_* \to +\infty$). Therefore one can write the boundary condition for the outgoing wave at the spatial infinity as

$$\psi(r) \sim e^{-\chi r_*} \quad as \quad r \to \infty \quad (r_* \to +\infty). \tag{20}$$

where $\chi = \sqrt{m^2 - \omega^2}$. Note that a bound state (decaying exponentially at spatial infinity) is characterized by $\omega^2 < m^2$ [3, 12, 13].

B. Behaviour of the effective potential

We present comparison of behaviour of the effective potentials of the stringy and RN BHs in Fig. 1 and Fig. 2. One can see from the Fig. 1 and Fig. 2 that the effective potentials of the stringy and RN BHs in tortoise coordinates are nearly the same for small values of the charge parameters q and e. Here, one should note that for the same values of the charge parameters $e = q$ the maximum height of the effective potential of the RN BH spacetime is a little bit higher than the one of the stringy BH spacetime. However, this maximum point of the effective potential of the RN spacetime is located closer to BH than the one of the stringy BH spacetime. This is due to the fact that increase in the value of the charge parameter decreases radius of the horizon of the RN BH while it does not change the horizon location of the stringy BH. With increasing value of the charge q, the height of the potential increases, however, the radius where the effective potential reaches its maximum is getting closer toward the horizon of the BH.

Copyright © 2022

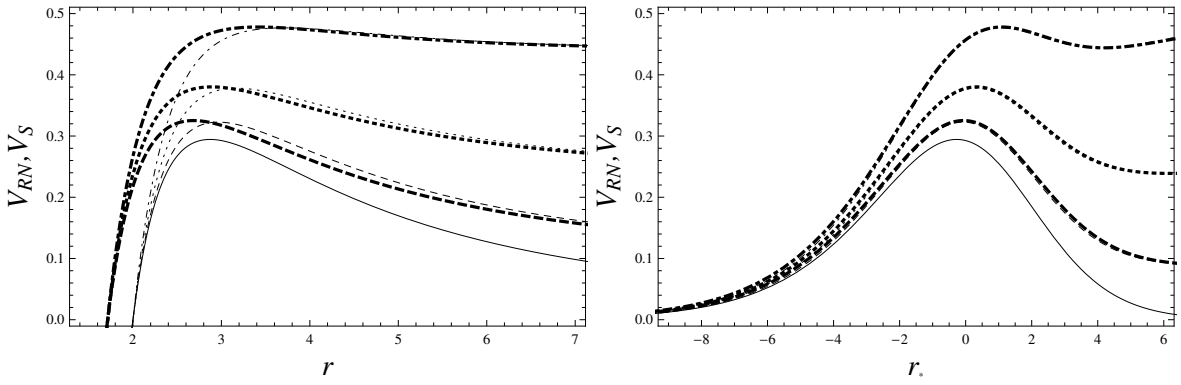


FIG. 1. Dependence of effective potentials of the stringy (thin) and RN (thick) BHs on the radial coordinate r (top) and tortoise coordinate r_* (bottom) for several values of the scalar field with mass m in the $\ell = 2$ mode. We set $m = 0$ (solid line), $m = 0.3$ (dashed lines), $m = 0.5$ (dotted lines) and $m = 0.7$ (dotdashed lines) in the case $q = e = 0.7$.

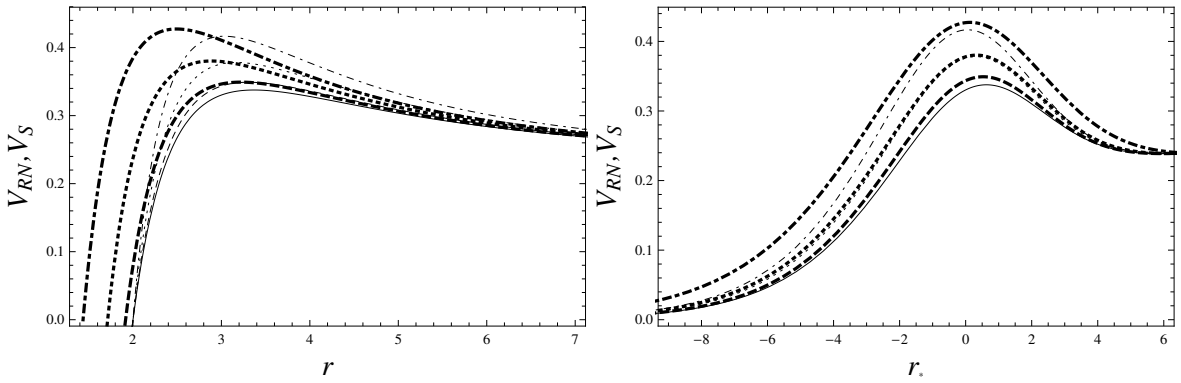


FIG. 2. Dependence of effective potentials of the stringy (thin) and RN (thick) BHs on the radial coordinate r (top) and tortoise coordinate r_* (bottom) for several values of the charge q, e for the case $q = e$ in the $\ell = 2$ mode. We set $m = 0.5$ and $q = e = 0$ (solid line), $q = e = 0.4$ (dashed lines), $q = e = 0.7$ (dotted lines) and $q = e = 0.9$ (dotdashed lines).

IV. QNM DETERMINED BY WKB METHOD

The Schrödinger-like wave equation (18) with the effective potential (14) cannot be solved analytically. Therefore, we have to look for numerical schemes for finding the QN frequencies. So far, several methods of solving the Schrödinger equation with effective potentials that do not allow for analytical solutions have been used [4–7]. One of them is the WKB method. The WKB method has several advantages over the other numerical methods of calculations: the wave function $\psi(r)$ has no divergence at the turning points so that this method gives opportunity to solve the Schrödinger-like wave equation for frequencies allowing many turning points at the effective potential; this method can be extended to higher orders to increase exactness; and finally, this method can be applied for all kinds of the potential. In order to calculate QN frequencies, we use the 6th order WKB method [16]:

$$\frac{i\left(\omega^2 - V(r_0)\right)}{\sqrt{-2V''(r_0)}} + \sum_{j=2}^{6} \Lambda_j = n + \frac{1}{2}\,, \tag{21}$$

where j is the order of the WKB corrections and Λ_j is the correction term corresponding to the jth order. One can find the expressions of Λ_j in [15, 45]. The prime "$'$" stands for the derivative with respect to the tortoise coordinate r_*.

We start calculating QN frequencies of the stringy BH in the case of massless scalar field, comparing them to the ones obtained for the RN BH. Quasinormal resonances of a charged scalar field in the RN BH spacetime were calculated in [12]. Here, in Tab. I these results are given for comparison. One can see from the Tab. I that for small values of the charge parameter, $q, e \lesssim 0.5$, the stringy and RN BHs behave similarly with respect to the QN frequencies.

Unlike the case of massless field effective potential, for the massive scalar field of the stringy BH the effective potential (14) does not tend to zero asymptotically, i.e.

$$V(r \to \infty) \to m^2\,. \tag{22}$$

Copyright © 2022

n	ℓ	$q=e=0.0$	$q=e=0.2$	$q=e=0.5$	$q=e=0.8$	$q=e=1.0$	$q=e=1.2$
0	1	0.2929 - 0.0976i	0.2949- 0.0980i	0.3062 - 0.0991i	0.3317 - 0.1013i	0.3624 - 0.1037i	0.4217 - 0.1061i
			0.2949 - 0.0980i	0.3065 - 0.0989i	0.3352 - 0.0991i	0.3777 - 0.0893i	-
	2	0.4836 - 0.0968i	0.4869 - 0.0970i	0.5054 - 0.0981i	0.5472 - 0.1005i	0.5988 - 0.1029i	0.6942 - 0.1059i
			0.4869 - 0.0970i	0.5060 - 0.0979i	0.5530 - 0.0983i	0.6266 - 0.0887i	-
	3	0.6754 - 0.0965i	0.6799 - 0.0967i	0.7057 - 0.0979i	0.7639 - 0.1003i	0.8359 - 0.1027i	0.9711 - 0.1056i
			0.6799 - 0.0967i	0.7065 - 0.0977i	0.7721 - 0.0981i	0.8761 - 0.0886i	-
	4	0.8674 - 0.0964i	0.8733 - 0.0966i	0.9063 - 0.0978i	0.9811 - 0.1002i	1.0735 - 0.1026i	1.2465 - 0.1056i
			0.8733 - 0.0966i	0.9073 - 0.0976i	0.9916 - 0.0980i	1.1259 - 0.0885i	-
1	2	0.4638 - 0.2956i	0.4673 - 0.2962i	0.4866 - 0.2994i	0.5301 - 0.3060i	0.5839 - 0.3126i	0.6674 - 0.3285i
			0.4673 - 0.2962i	0.4873 - 0.2988i	0.5372 - 0.2991i	0.6082 - 0.2691i	-
	3	0.6607 - 0.2923i	0.6653 - 0.2929i	0.6917 - 0.2963i	0.7513 - 0.3032i	0.8247 - 0.3103i	0.9613 - 0.3190i
			0.6654 - 0.2929i	0.6926 - 0.2957i	0.7604 - 0.2965i	0.8628 - 0.2672i	-
	4	0.8558 - 0.2909i	0.8617 - 0.2915i	0.8953 - 0.2949i	0.9711 - 0.3020i	1.0648 - 0.3092i	1.2311 - 0.3200i
			0.8618 - 0.2915i	0.8964 - 0.2944i	0.9823 - 0.2955i	1.1155 - 0.2664i	-
	5	1.0500 - 0.2901i	1.0573 - 0.2908i	1.0980 - 0.2943i	1.1901 - 0.3014i	1.3040 - 0.3086i	1.5184 - 0.3171i
			1.0573 - 0.2908i	1.0993 - 0.2937i	1.2036 - 0.2949i	1.3672 - 0.2660i	-
2	3	0.6336 - 0.4960i	0.6385 - 0.4970i	0.6660 - 0.5022i	0.7279 - 0.5128i	0.8043 - 0.5236i	0.9399 - 0.5405i
			0.6385 - 0.4969i	0.6671 - 0.5011i	0.7386 - 0.5009i	0.8368 - 0.4502i	-
	4	0.8337 - 0.4903i	0.8398 - 0.4913i	0.8743 - 0.4968i	0.9520 - 0.5080i	1.0479 - 0.5194i	1.1707 - 0.5587i
			0.8398 - 0.4913i	0.8755 - 0.4958i	0.9646 - 0.4966i	1.0950 - 0.4469i	-
	5	1.0315 - 0.4873i	1.0389 - 0.4884i	1.0804 - 0.4940i	1.1742 - 0.5055i	1.2900 - 0.5172i	1.5095 - 0.5301i
			1.0389 - 0.4883i	1.0818 - 0.4930i	1.1888 - 0.4944i	1.3503 - 0.4452i	-
	6	1.2278 - 0.4856i	1.2365 - 0.4866i	1.2852 - 0.4923i	1.3951 - 0.5040i	1.5309 - 0.5159i	1.7827 - 0.5308i
			1.2365 - 0.4866i	1.2868 - 0.4914i	1.4118 - 0.4930i	1.6041 - 0.4443i	-
3	4	0.8032 - 0.6975i	0.8095 - 0.6988i	0.8453 - 0.7059i	0.9257 - 0.7205i	1.0249 - 0.7353i	1.2114 - 0.7519i
			0.8096 - 0.6988i	0.8468 - 0.7045i	0.9400 - 0.7035i	1.0648 - 0.6319i	-
	5	1.0052 - 0.6899i	1.0127 - 0.6912i	1.0554 - 0.6988i	1.1515 - 0.7141i	1.2701 - 0.7297i	1.5002 - 0.7438i
			1.0128 - 0.6913i	1.0570 - 0.6974i	1.1676 - 0.6979i	1.3253 - 0.6275i	-
	6	1.2049 - 0.6854i	1.2137 - 0.6868i	1.2634 - 0.6945i	1.3753 - 0.7103i	1.5136 - 0.7264i	1.7583 - 0.7513i
			1.2137 - 0.6868i	1.2651 - 0.6932i	1.3934 - 0.6945i	1.5828 - 0.6250i	-
	7	1.4030 - 0.6825i	1.4130 - 0.6840i	1.4698 - 0.6918i	1.5978 - 0.7079i	1.7558 - 0.7243i	2.0408 - 0.7477i
			1.4131 - 0.6839i	1.4717 - 0.6905i	1.6178 - 0.6923i	1.8383 - 0.6234i	-

TABLE I. QNMs of the stringy (1st row) and RN (2nd row) BHs for the massless scalar field. The first column that corresponds to the case $q=e=0$ represents the QNMs for the Schwarzschild BH. The RN BH does not exist for $e>1$. This case corresponds to the RN naked singularities.

One can see from Fig. 1 that for small enough values of mass parameter m, the effective potential $V(r)$ is in the form of a barrier. However, with increasing value of m, asymptotical value of $V(r)$ (namely m^2) increases more rapidly than the peak of the potential. Consequently, in the case of $V(r_{max}) \leq m^2$, the effective potential is not in the form of barrier anymore. Therefore, in that case QNMs do not occur. To find the maximum value of the mass m allowing for existence of the potential barrier, we must solve the equation

$$V(r_{max}, m_{max}) - m^2_{max} = 0\,. \tag{23}$$

The results of the solution of Eq. (23) are illustrated in Fig. 3.

In the Tab. II and Fig. 3 values of mass m_{max} of the scalar field in the stringy (and RN) BH backgrounds are given for different values of the charge q (and e) and the multipole number ℓ. One can see from this Table that for small values of the charge q and e ($q, e \lesssim 0.5$) the maximum value of the mass of the scalar field m_{max} in the stringy BH is almost the same as those obtained for the RN BH.

However, we have to recall that with increasing value of the mass of the scalar field m, the accuracy of the WKB method decreases since for large mass m the turning points of the effective potential are located far away from each other due to broadening of the effective potential, and the radius where the effective potential reaches its maximum, r_0, shifts away from the event horizon of the BH. For the wave incoming from infinity towards the BH, the height of the potential barrier decreases. Vanishing of the peak of the effective potential implies that the potential is not able to trap the wave [46].

One can see from Fig. 3 that the values of the mass m_{max} of the scalar field that allow QNMs to occur in the stringy BH does not depend strongly on the charge parameter q, while it depends strongly on the multipole number ℓ.

The QNM frequency can be generally expressed in the form

$$\omega = Re(\omega) + iIm(\omega) \tag{24}$$

Copyright © 2022

ℓ	$q=e=0.0$	$q=e=0.2$	$q=e=0.4$	$q=e=0.6$	$q=e=0.8$	$q=e=1.0$	$q=e=1.2$
0	0.1925	0.1931	0.1951	0.1987	0.2045	0.2133	0.2277
		0.1931	0.1951	0.1985	0.2034	0.2089	-
1	0.3972	0.3992	0.4053	0.4164	0.4343	0.4629	0.5137
		0.3992	0.4054	0.4169	0.4365	0.4725	-
2	0.6378	0.6411	0.6511	0.6693	0.6987	0.7463	0.8314
		0.6411	0.6512	0.6702	0.7027	0.7640	-
3	0.8841	0.8885	0.9025	0.9278	0.9688	1.0351	1.1544
		0.8885	0.9027	0.9291	0.9744	1.0605	-
4	1.1320	1.1377	1.1556	1.1881	1.2406	1.3258	1.4792
		1.1377	1.1558	1.1897	1.2479	1.3587	-

TABLE II. Maximum values of the mass of the scalar field m_{max} allowing existence of QNM in the field of the stringy BH (1st row) and the RN BH (2nd row). The case of $q=e=0$ corresponds to the Schwarzschild BH. A sign "-" stands when no QNM exists for the value of the multipole number ℓ and the charge q.

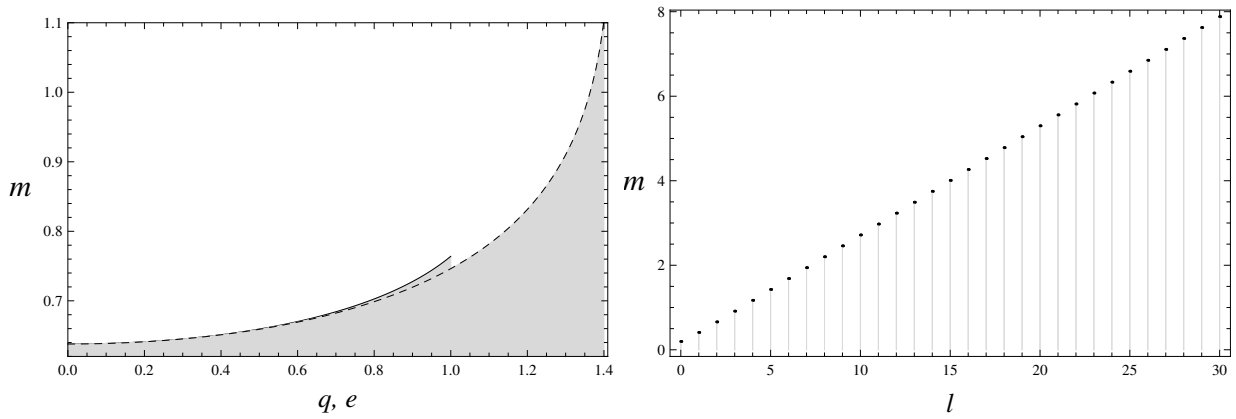


FIG. 3. Possible values of the scalar field mass m_{max} that give the limit of existence of QNMs in the field of stringy BH (dashed) and RN one (solid). Shaded region represents part of parameter space where the QNM can occur. In the white region there are no QNM. Top panel is for $\ell=2$ mode. In the bottom panel also limiting values of the scalar field mass m_{max} enabling existence of QNMs in the field of stringy and RN BHs are given in dependence on the multipole number ℓ in the case of $q=e=0.5$.

where $Re(\omega)$ is the real oscillation frequency, and $Im(\omega)$ is the imaginary oscillation frequency that represents damping or enhancing of the oscillatory mode.

V. QNM IN LARGE MULTIPOLE NUMBER LIMIT

It is known that the WKB method has a very good accuracy for large values of ℓ. Then, the QN frequencies tend to a limited value. In order to find the QN frequencies for large ℓ, we expand the first order WKB approximation expression in powers of $1/\ell$. We arrive at relations

$$
\begin{aligned}
&Re(\omega)=\left[\frac{r_0-2}{r_0^2(r_0-q^2)}\right]^{1/2}\left(\ell+\frac{1}{2}\right)+O\left(\frac{1}{\ell}\right),\\
&Im(\omega)=-\frac{1}{r_0^2(r_0-q^2)}\left[q^4(r_0^2-9r_0+16)-\right.\\
&\left.q^2r_0(3r_0^2-25r_0+42)+r_0^2(3r_0^2-20r_0+30)\right]^{1/2}\\
&\times\left(n+\frac{1}{2}\right)+O\left(\frac{1}{\ell}\right),
\end{aligned}
\tag{25}
$$

Copyright © 2022

m	n	ℓ	$q=e=0.0$	$q=e=0.2$	$q=e=0.5$	$q=e=0.8$	$q=e=1.0$	$q=e=1.2$
0.3	0	1	0.3337-0.0717i	0.3353-0.0723i	0.3444-0.0754i	0.3654-0.0813i	0.3920-0.0872i	0.4432-0.0946i
				0.3353-0.0723i	0.3447-0.0753i	0.3684-0.0803i	0.4047-0.0783i	-
		2	0.5123-0.0868i	0.5153-0.0872i	0.5321-0.0891i	0.5705-0.0929i	0.6186-0.0967i	0.7095-0.1015i
				0.5153-0.0871i	0.5326-0.0889i	0.5759-0.0912i	0.6441-0.0849i	-
		3	0.6967-0.0913i	0.7010-0.0916i	0.7256-0.0932i	0.7812-0.0963i	0.8505-0.0995i	0.9825-0.1033i
				0.7011-0.0916i	0.7263-0.0930i	0.7890-0.0944i	0.8888-0.0866i	-
	1	2	0.4782-0.2742i	0.4816-0.2750i	0.5004-0.2797i	0.5429-0.2891i	0.5952-0.2986i	0.6862-0.3133i
				0.4816-0.2750i	0.5012-0.2792i	0.5503-0.2831i	0.6214-0.2590i	-
		3	0.6761-0.2791i	0.6806-0.2799i	0.7063-0.2843i	0.7642-0.2930i	0.8360-0.3019i	0.9782-0.3103i
				0.6806-0.2799i	0.7071-0.2838i	0.7732-0.2870i	0.8739-0.2617i	-
		4	0.8697-0.2823i	0.8755-0.2831i	0.9084-0.2871i	0.9826-0.2954i	1.0745-0.3037i	1.2479-0.3138i
				0.8756-0.2830i	0.9094-0.2866i	0.9937-0.2893i	1.1247-0.2629i	-
	2	3	0.6407-0.4804i	0.6456-0.4815i	0.6730-0.4877i	0.7347-0.5003i	0.8105-0.5130i	0.9903-0.5082i
				0.6456-0.4815i	0.6742-0.4867i	0.7457-0.4890i	0.8451-0.4422i	-
		4	0.8428-0.4787i	0.8489-0.4798i	0.8830-0.4861i	0.9600-0.4989i	1.0549-0.5119i	1.2318-0.5280i
				0.8489-0.4798i	0.8843-0.4852i	0.9727-0.4880i	1.1030-0.4416i	-
		5	1.0409-0.4787i	1.0481-0.4798i	1.0893-0.4861i	1.1821-0.4988i	1.2968-0.5117i	1.5105-0.5277i
				1.0482-0.4798i	1.0907-0.4851i	1.1967-0.4880i	1.3574-0.4416i	-
0.5	0	1	-	-	-	-	-	0.4560-0.0737i
			-	-	-	-	0.4173-0.0403i	-
		2	0.5649-0.0676i	0.5673-0.0683i	0.5810-0.0716i	0.6132-0.0782i	0.6547-0.0848i	0.7382-0.0930i
				0.5673-0.0683i	0.5814-0.0716i	0.6175-0.0774i	0.6761-0.0769i	-
		3	0.7353-0.0818i	0.7392-0.0822i	0.7614-0.0845i	0.8125-0.0890i	0.8769-0.0936i	0.9998-0.0994i
				0.7392-0.0822i	0.7620-0.0844i	0.8194-0.0876i	0.9118-0.0828i	-
	1	2	0.5026-0.2347i	0.5058-0.2361i	0.5240-0.2433i	0.5647-0.2577i	0.6148-0.2723i	0.7268-0.2841i
				0.5058-0.2361i	0.5248-0.2430i	0.5725-0.2533i	0.6440-0.2398i	-
		3	0.7034-0.2549i	0.7078-0.2560i	0.7321-0.2621i	0.7873-0.2743i	0.8560-0.2865i	0.9701-0.3067i
				0.7078-0.2560i	0.7330-0.2617i	0.7962-0.2694i	0.8937-0.2513i	-
		4	0.8946-0.2667i	0.9002-0.2677i	0.9317-0.2729i	1.0031-0.2834i	1.0921-0.2940i	1.2627-0.3066i
				0.9002-0.2677i	0.9327-0.2725i	1.0139-0.2781i	1.1411-0.2567i	-
	2	3	0.6534-0.4523i	0.6582-0.4538i	0.6854-0.4617i	0.7463-0.4777i	0.8211-0.4939i	0.8678-0.5692i
				0.6583-0.4538i	0.6866-0.4608i	0.7580-0.4674i	0.8598-0.4275i	-
		4	0.8589-0.4576i	0.8649-0.4590i	0.8984-0.4668i	0.9741-0.4824i	1.0675-0.4981i	1.2525-0.5135i
				0.8649-0.4590i	0.8997-0.4660i	0.9870-0.4724i	1.1166-0.4321i	-
		5	1.0575-0.4631i	1.0647-0.4644i	1.1050-0.4718i	1.1962-0.4867i	1.3091-0.5017i	1.5123-0.5233i
				1.0647-0.4644i	1.1064-0.4710i	1.2108-0.4767i	0.3697-0.4350i	-
0.8	0	2	-	-	-	-	-	0.8042-0.0687i
				-	-	-	0.7582-0.0486i	-
		3	0.8331-0.0560i	0.8359-0.0568i	0.8522-0.0611i	0.8914-0.0694i	0.9435-0.0777i	1.0494-0.0883i
				0.8360-0.0568i	0.8527-0.0611i	0.8964-0.0691i	0.9702-0.0720i	-
	1	2	-	-	-	-	-	0.7141-0.2352i
			-	-	-	-	-	-
		3	0.7677-0.1898i	0.7716-0.1920i	0.7936-0.2032i	0.8428-0.2249i	0.9043-0.2460i	1.0218-0.2736i
				0.7716-0.1920i	0.7945-0.2032i	0.8513-0.2226i	0.9414-0.2230i	-
		4	0.9561-0.2266i	0.9610-0.2282i	0.9892-0.2365i	1.0538-0.2528i	1.1355-0.2690i	1.2918-0.2898i
				0.9610-0.2282i	0.9901-0.2362i	1.0638-0.2492i	1.1815-0.2400i	-
	2	3	0.6593-0.3917i	0.6682-0.3928i	0.7082-0.4009i	0.7733-0.4222i	0.8457-0.4459i	0.9721-0.4827i
				0.6683-0.3928i	0.7097-0.4002i	0.7861-0.4139i	0.8913-0.3898i	-
		4	0.8975-0.4046i	0.9032-0.4067i	0.9353-0.4180i	1.0078-0.4407i	1.0973-0.4635i	1.2572-0.4961i
				0.9032-0.4067i	0.9367-0.4174i	1.0211-0.4330i	1.1496-0.4074i	-
		5	1.0980-0.4238i	1.1048-0.4257i	1.1433-0.4359i	1.2305-0.4563i	1.3390-0.4767i	1.5424-0.5029i
				1.1049-0.4257i	1.1447-0.4353i	1.2450-0.4480i	1.3998-0.4180i	-
1.0	0	3	-	-	-	-	1.0082-0.0602i	1.0961-0.0767i
			-	-	-	0.9715-0.0479i	1.0277-0.0592i	-
	1	2	-	-	-	-	-	-
		3	-	-	-	-	0.9401-0.2017i	1.0532-0.2449i
			-	-	-	-	0.9820-0.1912i	-
		4	1.0131-0.1862i	1.0175-0.1883i	1.0426-0.1998i	1.1009-0.2222i	1.1759-0.2441i	1.3240-0.2721i
				1.0175-0.1883i	1.0435-0.1998i	1.1102-0.2203i	1.2191-0.2227i	-
	2	3	-	-	-	-	0.6869-0.4085i	0.9704-0.4505i
			-	-	-	-	0.8607-0.3428i	-
		4	0.9271-0.3536i	0.9332-0.3564i	0.9664-0.3713i	1.0375-0.4007i	1.1240-0.4302i	1.2915-0.4671i
				0.9333-0.3564i	0.9678-0.3710i	1.0512-0.3949i	1.1788-0.3829i	-
		5	1.1351-0.3858i	1.1416-0.3883i	1.1784-0.4013i	1.2620-0.4270i	1.3664-0.4527i	1.5598-0.4869i
				1.1417-0.3883i	1.1798-0.4009i	1.2764-0.4205i	1.4273-0.4014i	-

TABLE III. QNMs of stringy (1st row) and RN (2nd row) BHs for massive scalar field.

Copyright © 2022

TABLE IV. The eikonal limit for QNMs of the stringy BH when $q = \sqrt{2} - \epsilon$.

ϵ	r_0	$\frac{Re(\omega)}{\ell+1/2}$	$\frac{Im(\omega)}{n+1/2}$
10^{-1}	2.4586	0.3221	-0.2108
10^{-3}	2.0525	0.4746	-0.1080
10^{-5}	2.0053	0.4973	-0.0362
~ 0	~ 2	~ 0.5	~ 0

where r_0 is the radius at which the effective potential reaches its maximum, given by the formula

$$r_0 = \frac{1}{4}\left(6 + q^2 + \sqrt{(q^2-2)(q^2-18)}\right). \tag{26}$$

If $q \to 0$, the stringy BH spacetime reduces to the Schwarzschild one and $r_0 \to 3$ that corresponds to the radius of the photon circular orbit [47], and the eikonal limit (25) for the Schwarzschild BH reads [45]

$$\begin{aligned} \lim_{q\to 0} Re(\omega) &= \frac{1}{3\sqrt{3}}\left(\ell + \frac{1}{2}\right), \\ \lim_{q\to 0} Im(\omega) &= -\frac{1}{3\sqrt{3}}\left(n + \frac{1}{2}\right). \end{aligned} \tag{27}$$

In our case, as mentioned above, the value of the charge is restricted by the condition $q < \sqrt{2}$. The reason of excluding the case of $q > \sqrt{2}$ is that in this case event horizon is surrounded by the singular surface and we exclude from our consideration the naked singularity spacetimes.

Interestingly, with increase of the value of the charge q, the eikonal limit of the real part of the QN frequency in the stringy BH increases relative to the Schwarzschild one, while the imaginary part of QN frequency decreases to zero. When $q^2 = 2$, there is no damping, namely QN frequency has only real part. Contribution of the mass of the scalar field m is negligible, because the corresponding term is of the order of $O(1/\ell)$.

The eikonal limit of the QNM of the RN BH reads

$$\begin{aligned} Re(\omega_{RN}) &= \frac{1}{r_0^2}\left[r_0(r_0-2)+e^2\right]^{1/2}\left(\ell+\frac{1}{2}\right) + O\left(\frac{1}{\ell}\right), \\ Im(\omega_{RN}) &= -\frac{1}{r_0^3}\left[14e^4 + 3e^2 r_0(5r_0-14) + \right. \\ &\left. r_0^2(3r_0^2 - 20r_0 + 30)\right]^{1/2}\left(n+\frac{1}{2}\right) + O\left(\frac{1}{\ell}\right), \end{aligned} \tag{28}$$

where [48]

$$r_0 = \frac{1}{2}\left(3 + \sqrt{9 - 8e^2}\right). \tag{29}$$

When $e \to 0$, the RN BH coincides with the Schwarzschild one and $r_0 \to 3$. In the extremal RN BH case $e \to 1$ and $r_0 \to 2$; then the eikonal limit (28) takes the form

$$\begin{aligned} \lim_{e\to 1} Re(\omega_{RN}) &= \frac{1}{4}\left(\ell + \frac{1}{2}\right), \\ \lim_{e\to 1} Im(\omega_{RN}) &= -\frac{1}{4\sqrt{2}}\left(n + \frac{1}{2}\right). \end{aligned} \tag{30}$$

In Fig. 4, we compare the behaviour of the maximum point of the effective potentials of the stringy and RN BHs in dependence on the charge parameters q and e, respectively. From the eikonal limits for QNMs of the stringy and RN BHs, we can conclude that in the extremal case ($q, e \to q_{max}, e_{max}$), $r_0 \to 2$ for both BHs.

Thus, we can say that for large values of the multipole number ℓ, in the stringy BH the scalar field can oscillate in QNM with higher real frequencies and with smaller damping rates in comparison to the Schwarzschild and RN BHs. Namely, QN frequencies of scalar field around the stringy BH are longer living than the ones occuring in the Schwarzschild and RN BHs. Furthermore, one can see from the Tab. III and the expressions of QNMs of the stringy (25) and RN (28) BHs for the large multipole number ℓ that lower QNMs strongly depend on the mass of the scalar field m, however asymptotic behavior of QNMs do not depend on the mass of the field m and they are the same as those related to the massless case.

Copyright © 2022

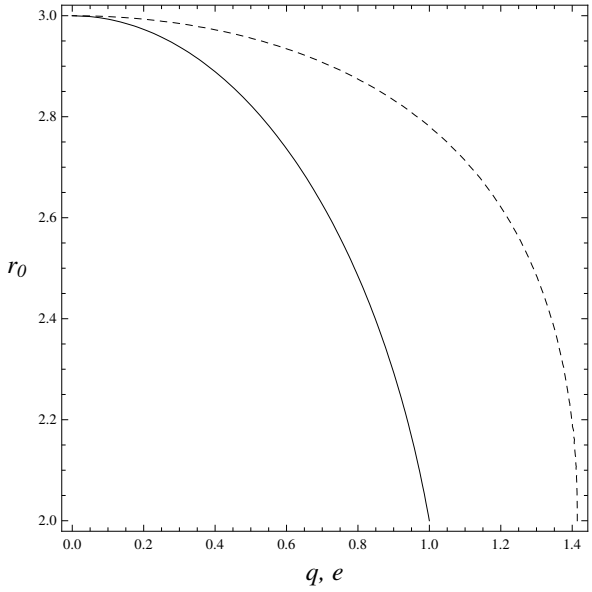


FIG. 4. Dependence of radius r_0 where the effective potential reaches its maximum on the charge q and e for stringy (dashed) and RN (solid) BHs, respectively in the case of limit of large ℓ.

VI. STABILITY

Stability of perturbative test fields is one of the crucial issues related to BHs. An instability could have a dramatic consequences and breakdown of the test-field limit. Since we have the Schrödinger-like wave equation (18), we can study stability problem of the scalar fields from that. We have to keep in our considerations that if QNMs decay in time, the BH is stable, if there is any growing mode, the BH could be unstable against small perturbations. In order to check the stability of the stringy BH we multiply the Schrödinger-like wave equation (18) by complex conjugate of the wave function $\psi(r)$

$$\psi^*(r_*)\frac{d^2\psi(r_*)}{dr_*^2}+\omega^2\psi(r_*)\psi^*(r_*)-V(r_*)\psi(r_*)\psi^*(r_*)=0 \tag{31}$$

and integrate equation (31) across the whole range of the tortoise coordinate r_*

$$\int_{-\infty}^{+\infty}\left[\left(\omega^2-V(r_*)\right)|\psi(r_*)|^2-\left|\frac{\psi(r_*)}{dr_*}\right|^2\right]dr_*+ \psi^*(r_*)\frac{\psi(r_*)}{dr_*}\Big|_{-\infty}^{+\infty}=0\,. \tag{32}$$

In order to guarantee the stability of the scalar fields, imaginary part of the QN frequency must be negative, $Im(\omega)<0$ [35]. Now, taking into account the boundary conditions (19) and (20), and the fact that the effective potential $V(r_*)$ is always positive, we write the imaginary part of above integral (32)

$$Re(\omega)\left[|\psi(+\infty)|^2+|\psi(-\infty)|^2+2Im(\omega) \times\int_{-\infty}^{+\infty}|\psi(r_*)|^2\,dr_*\right]=0\,, \tag{33}$$

Here, real oscillations cannot be zero, i.e. $Re(\omega)\neq 0$. Therefore, according to Eq. (33), the other part of the equation must be zero. Since that we can find the expression for the imaginary part of the QN frequency in the form:

$$Im(\omega)=-\frac{|\psi(+\infty)|^2+|\psi(-\infty)|^2}{2\int_{-\infty}^{+\infty}|\psi(r_*)|^2\,dr_*}<0\,. \tag{34}$$

Copyright © 2022

Thus, we can conclude that the imaginary part of the QN frequency is always negative, $Im(\omega) < 0$. This means that the stringy BH does not allow for existence of oscillating unstable modes. Moreover, from the positivity of the effective potential $V(r_*)$ in the whole range of the tortoise coordinate r_* one can say that stringy BHs are stable under scalar perturbations [36]. It has been proven in the papers [37] that the RN BH is also stable under scalar perturbations.

VII. SCATTERING

In this section we study the greybody factor for the stringy BH. Greybody factor is understood as the probability for an outgoing wave in ω-mode, to reach infinity or equivalently, the absorption probability for an incoming wave in ω-mode that is absorbed by the BH [38, 39]. In other words, the greybody factor is the tunneling probability of the wave through the barrier determined by the effective potential in the given spacetime.

In order to calculate the greybody factor we write the boundary conditions for the ingoing and outgoing waves that are the solution of the Schrödinger-like wave equation (18) given in the asymptotic form

$$\begin{aligned} \psi_\omega &= e^{-i\omega r_*} + R(\omega)e^{i\omega r_*}, \quad at \quad r_* \to +\infty, \\ \psi_\omega &= T(\omega)e^{-i\omega r_*}, \qquad\quad at \quad r_* \to -\infty, \end{aligned} \tag{35}$$

where $R(\omega)$ and $T(\omega)$ are the reflection and transmission coefficients, respectively. We write the above given boundary conditions (35) for $\omega \to -\omega$:

$$\begin{aligned} \psi_{-\omega} &= e^{i\omega r_*} + R(-\omega)e^{-i\omega r_*}, \quad at \quad r_* \to +\infty, \\ \psi_{-\omega} &= T(-\omega)e^{i\omega r_*}, \qquad\quad at \quad r_* \to -\infty. \end{aligned} \tag{36}$$

From these two boundary conditions we can write the expression for the flux [40]

$$J = \frac{1}{2i}\left[\psi_{-\omega}\frac{d\psi_\omega}{dr_*} - \psi_\omega\frac{d\psi_{-\omega}}{dr_*}\right]. \tag{37}$$

Using the boundary conditions (35) and (36), we find the relation between the reflection and transmission coefficients from the flux conservation in the form

$$R(\omega)R(-\omega) + T(\omega)T(-\omega) = 1\,. \tag{38}$$

If we consider ω real ($\omega \in \mathbb{R}$), we can write that $\psi_{-\omega} = \psi^*_\omega$, $R(-\omega) = R^*(\omega)$ and $T(-\omega) = T^*(\omega)$. Then the relation (38) can be written in the form

$$|R|^2 + |T|^2 = 1\,. \tag{39}$$

A wave with frequency ω larger than the height of the potential barrier V_0 will not be (classically) reflected by the barrier. Therefore, in this case reflection coefficient is close to zero. And the incoming wave with smaller frequency than the height of the potential barrier, $\omega^2 < V_0$, is reflected partly, while the rest part is transmitted through the barrier by tunneling effect, depending on the values of ω and V_0. This is why this case is more interesting to study.

First, we consider the small frequency case when ω^2 is much less than the height of the potential barrier V_0 ($\omega^2 \ll V_0$). For such small values of ω^2, the WKB approximation has not high accuracy because of the large distance between two turning points. In this case transmission coefficient is given by the well-known formula

$$T = e^{-\int_{r_{*1}}^{r_{*2}} dr_* \sqrt{V(r_*)-\omega^2}}, \quad as \quad \omega^2 \ll V_0\,, \tag{40}$$

and the reflection coefficient

$$R = \left(1 - e^{-2\int_{r_{*1}}^{r_{*2}} dr_* \sqrt{V(r_*)-\omega^2}}\right)^{1/2}, \quad as \quad \omega^2 \ll V_0\,. \tag{41}$$

The radii r_{*1} and r_{*2} are the classical turning points that are the solutions of the equation $V(r_*) = \omega^2$. At the small values of ω, transmission coefficient is close to zero while the reflection coefficient is close to one [41].

The second limit case is that the value of ω^2 is of the same order as the maximum height of the potential barrier V_0, i.e. $\omega^2 \approx V_0$. Here, we can calculate the greybody factor by using the sixth order WKB approximation because of the small distance between the turning points [39, 42]. Then we arrive at

$$R = \left(1 + e^{-2i\pi(n+1/2)}\right)^{-1/2}, \tag{42}$$

Copyright © 2022

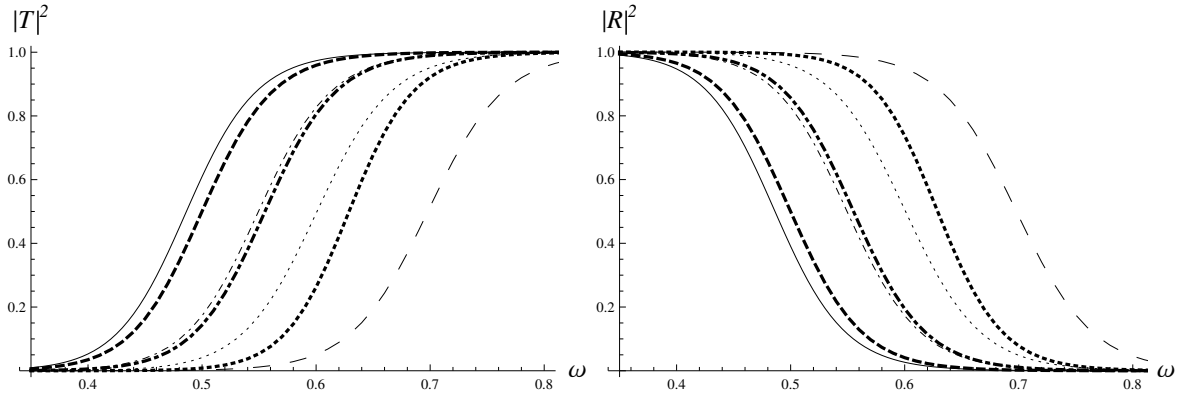


FIG. 5. Transmission (top panel) and reflection (bottom panel) coefficients for scalar field $\ell = 2$ mode of the stringy (thin) and RN (thick) BHs for several values of the charge parameters q and e, respectively. Where we set the following values for the charges: $q = e = 0$ (solid line. This corresponds to the one of the Schwarzschild BH), $q = e = 0.4$ (dashed), $q = e = 0.8$ (dotdashed), $q = e = 1$ (dotted) and $q = 1.2$ (large dashed).

where $(n + 1/2)$ is given by the formula of the sixth order WKB method (21). From (39) with (42) one can write the expression for the transmission coefficient as

$$|T|^2 = 1 - \left| \left(1 + e^{-2i\pi(n+1/2)}\right)^{-1/2} \right|^2 . \tag{43}$$

In Fig. 5, we give the reflection and transmission coefficients for the scalar fields in the spacetimes of the stringy and RN BHs for several values of the charge parameters q and e, respectively, in the mode $\ell = 2$.

One can see from Fig. 5 that the scalar field in the stringy BH background is lower than in the Schwarzschild BH, being higher than in the RN BH spacetimes. For large values of the charges ($q = e \gtrsim 0.5$), the reflection of the wave is larger in the RN spacetime than in the stringy spacetime, while for small enough values of the charges ($q = e \lesssim 0.5$), the behaviour is similar in the RN and stringy BHs spacetimes for reflecting and transmitting waves. Of course, the stringy BHs can be better reflectors due to the larger range of values of the charge allowing for existence of BHs. The increase in the value of charge q decreases probability of the transmission of the wave.

VIII. CONCLUSION

We have studied the QNMs of the massive and massless scalar fields in the stringy BH spacetimes comparing the results to those obtained for the RN BH spacetimes. It has been shown that increasing charge parameter of the stringy BH increases both parts (real and imaginary) of the QN frequency. We have shown that for small values of the charge parameters of the stringy and RN BHs ($q = e \lesssim 0.5$) the scalar field oscillates with nearly the same QN frequencies. For values of the charge parameters $q = e > 0.5$, the real and imaginary parts of the QN frequencies for the stringy BHs keep increasing, the real part of the QN frequencies for the RN BHs also keeps increasing, while the imaginary part starts decreasing rapidly for the values $e \gtrsim 0.7$. The QNMs of the massive scalar field vanish when the mass of the scalar field exceeds certain value depending on the spacetime charge q and the multipole number ℓ representing the angular momentum of a scalar wave. Mass of the scalar field increases the frequency of the real oscillations and decreases the imaginary part of QN frequency (damping rate). Therefore we can say that mass of the scalar field makes QNMs longer lived. Moreover, we have shown that for the large values of the multipole number ℓ the real part of the QN frequency in the stringy BH increases relative to the Schwarzschild one, while the imaginary part of QN frequency decreases to zero when the charge parameter approaches its extreme value.

Furthermore, it has been shown that the stringy BHs are stable against small perturbations.

The greybody factor (transmission and reflection of incoming wave) has been calculated. The greybody factors of the stringy and RN BHs are also very similar for small values of the charge parameters ($q = e \lesssim 0.5$). We have shown that both stringy and RN BHs are better wave reflectors in comparison to the Schwarzschild BHs. In the highly charged cases ($q = e \gtrsim 0.5$) RN BHs are better than the stringy BHs in reflecting the scalar waves, however, the stringy BHs can be better reflector than the RN BHs in the case of large values of the charge parameter $q > 1$.

We can conclude that for large values of the dimensionless charge parameters ($q, e > 0.5$) the quasinormal oscillatory modes

Copyright © 2022

and scattering of scalar waves enable to distinguish easily the stringy and RN BHs.

[1] T. Regge and J. A. Wheeler, Phys. Rev. **108**, 1063 (1957);
D. R. Brill and J. A. Wheeler, Rev. Mod. Phys. **29**, 465 (1957).
[2] V. P. Frolov and I. D. Novikov, *Black Hole Physics: Basic Concepts and New Developments* (Dordrecht: Kluwer Academic, 1998).
[3] J. Bičák, Z. Stuchlík, and M. Šob, Czech. J. Phys. **28**, 121 (1978).
[4] H. P. Nollert, Classical Quantum Gravity **16**, R159 (1999).
[5] K. D. Kokkotas and B. G. Schmidt, Living Rev. Rel. **2**, 2 (1999);
A. Nagar and L. Rezzolla, Classical Quantum Gravity **22**, R167 (2005).
[6] E. Berti, V. Cardoso, and A. O. Starinets, Classical Quantum Gravity **26**, 163001 (2009).
[7] R. A. Konoplya and A. Zhidenko, Rev. Mod. Phys. **83**, 793 (2011).
[8] E. W. Leaver, Proc. Roy. Soc. Lond. A **402**, 285 (1985);
S. Iyer, Phys. Rev. D **35**, 3632 (1987).
[9] K. D. Kokkotas and B. F. Schutz, Phys. Rev. D **37**, 3378 (1988).
[10] E. W. Leaver, Phys. Rev. D **41**, 2986 (1990).
[11] N. Andersson and H. Onozawa, Phys. Rev. D **54**, 7470 (1996).
[12] S. Hod, Phys. Rev. Lett. **81**, 4293 (1998); Phys. Lett. B **710**, 349 (2012);
[13] R. Konoplya, Phys. Lett. B **555**, 117 (2002).
[14] J. F. Chang and Y. G. Shen, Int. J. Theor. Phys. **46**, 1570 (2007).
[15] S. Iyer and C. M. Will, Phys. Rev. D **35**, 3621 (1987).
[16] R. A. Konoplya, Phys. Rev. D **68**, 124017 (2003); J. Phys. Stud. **8**, 93 (2004).
[17] G. Gibbons and K. Maeda, Nucl. Phys. B **298**, 741 (1988).
[18] D. Garfinkle, G. T. Horowitz, and A. Strominger, Phys. Rev. D **43**, 3140 (1991).
[19] C. F. E. Holzhey and F. Wilczek, Nucl. Phys. B **380**, 447 (1992).
[20] V. Ferrari, M. Pauri, and F. Piazza, Phys. Rev. D **63**, 064009 (2001).
[21] F.-W. Shu and Y.-G. Shen, Phys. Rev. D **70**, 084046 (2004).
[22] S. Chen and J. Jing, Classical Quantum Gravity **22**, 1129 (2005).
[23] S. Chen and J. Jing, Classical Quantum Gravity **22**, 533 (2005).
[24] M. Azreg-Aïnou, Classical Quantum Gravity **245**, 16 (1999).
[25] R. A. Konoplya, Phys. Rev. D **66**, 084007 (2002); Gen. Rel. Grav. **34**, 329 (2002).
[26] S. Chen and J. Jing, Classical Quantum Gravity **22**, 4651 (2005);
S. W. Wei, Y. X. Liu, K. Yang, and Y. Zhong, Phys. Rev. D **81**, 104042 (2010).
[27] A. J. M. Medved, D. Martin, and M. Visser, Classical Quantum Gravity **21**, 1393 (2004);
B. Toshmatov, Z. Stuchlík, B. Ahmedov, and D. Malafarina, Phys. Rev. D **99**, 064043 (2019).
[28] R. Li, Phys. Rev. D **88**, 127901 (2013).
[29] R. Li, Y. Tian, H. Zhang, and J. Zhao, arXiv:1506.04267 [gr-qc].
[30] R. Li and J. Zhao, Eur. Phys. J. C **74**, 3051 (2014);
B. Toshmatov, Z. Stuchlík, and B. Ahmedov, Phys. Rev. D **98**, 085021 (2018).
[31] R. Li and J. Zhao, Phys. Lett. B **740**, 317 (2015).
[32] R. Li, J. Zhao, X. Wu, and Y. Zhang, Eur. Phys. J. C **75**, 142 (2015).
[33] S. Hod, Phys. Lett. B **713**, 505 (2012); Phys. Lett. B **739**, 157 (2014).
[34] W. Kim and J. J. Oh, J. Korean Phys. Soc. **52**, 986 (2008).
[35] B. Toshmatov, Z. Stuchlík, J. Schee, and B. Ahmedov, Phys. Rev. D **98**, 084058 (2018);
S. Fernando and C. Holbrook, Int. Jour. Theor. Phys. **45**, 1630 (2004);
M. Kimura, K. Murata, H. Ishihara, and J. Soda, Phys. Rev. D **77**, 064015 (2008).
[36] S. Chandrasekhar, *The Mathematical Theory of Black Holes* (Oxford University Press, New York, 1983).
[37] S. Hod, Phys. Lett. B **718**, 1489 (2013); Phys. Rev. D **91**, 044047 (2015).
[38] V. Cardoso, M. Cavaglia, and L. Gualtieri, Phys. Rev. Lett. **96**, 071301 (2006).
[39] R. A. Konoplya and A. Zhidenko, Phys. Rev. D **81**, 124036 (2010); Phys. Lett. B **686**, 199 (2010).
[40] T. R. Choudhury and T. Padmanabhan, Phys. Rev. D **69**, 064033 (2004);
T. Harmark, J. Natario, and R. Schiappa, Adv. Theor. Math. Phys. **14**, 727 (2010).
[41] P. Boonserm and M. Visser, Phys. Rev. D **78**, 101502 (2008).
[42] B. Toshmatov, A. Abdujabbarov, Z. Stuchlík, and B. Ahmedov, Phys. Rev. D **91**, 083008 (2015);
B. Toshmatov, C. Bambi, B. Ahmedov, Z. Stuchlík, and J. Schee, Phys. Rev. D **96**, 064028 (2017).
[43] A. Zhidenko, arXiv:0903.3555.
[44] D. Ida, K. Y. Oda, and S. C. Park, Phys. Rev. D **67**, 064025 (2003) [Erratum-ibid. D **69**, 049901 (2004)].
[45] V. Ferrari and B. Mashhoon, Phys. Rev. Lett. **52**, 1361 (1984);
R. A. Konoplya, Phys. Rev. D **68**, 024018 (2003).
[46] A. Ohashi and M. Sakagami, Classical Quantum Gravity **21**, 3973 (2004);
B. Toshmatov and Z. Stuchlík, Eur. Phys. J. Plus **132**, 324 (2017).

Copyright © 2022

[47] Z. Stuchlík, Bull. Astron. Inst. Czech. **34**, 129 (1983).
[48] Z. Stuchlík and S. Hledik, Acta Phys. Slovaca, **52**, 363 (2002).

Copyright © 2022